ARTICLE

Imaging the [1+1] Two-Photon Dissociation Dynamics of Br_2^+ in a Cold Ion Beam

Hao Liang, Zheng-fang Zhou, Ze-feng Hua, Yun-xiao Zhao, Shao-wen Feng, Yang Chen*, Dong-feng Zhao*

Hefei National Laboratory for Physical Sciences at the Microscale, and Department of Chemical Physics, University of Science and Technology of China, Hefei 230026, China

(Dated: Received on April 28, 2019; Accepted on June 6, 2019)

The [1+1] two-photon dissociation dynamics of mass-selected $^{79}Br_2^+$ has been studied in a cold ion beam using a cryogenic cylindrical ion trap velocity map imaging spectrometer. The quartet $1^4\Sigma^-_{u,3/2}$ state of $^{79}Br_2^+$ is employed as an intermediate state to initiate resonance enhanced two-photon excitation to high-lying dissociative states in the 4.0−5.0 eV energy region above the ground rovibronic state. Total kinetic energy release (TKER) and the two-dimensional recoiling velocity distributions of fragmented $^{79}Br^+$ ions are measured using the technique of DC-slice velocity map imaging. Branching ratios for individual state-resolved product channels are determined from the TKER spectra. The measured photofragment angular distributions indicate that the dissociation of $^{79}Br_2^+$ occurs in dissociative Ω=3/2 states via $\Delta\Omega$=0 parallel transitions from the $1^4\Sigma^-_{u,3/2}$ intermediate state. Due to the considerable spin-orbit coupling effects in the excited states of $^{79}Br_2^+$, higher-lying dissociative quartet states are likely responsible for the observed photodissociation processes.

Key words: Photodissociation dynamics, Br_2^+, Velocity map imaging, Ion trap

I. INTRODUCTION

Photochemistry of halogen molecules and organic halides has long been a hot topic of gas-phase physical chemistry because of the important role they play in Earth's atmosphere and in the formation of secondary organic aerosols [1–5]. The halogen-containing molecules also serve as prototypical model systems in understanding light induced phenomena in molecular physics, such as spin-orbit coupling effect, $\pi\sigma^*/n\sigma^*$ state excitation and dynamics [6, 7]. In recent years, extensive experimental and theoretical studies [8–25] on the photodissociation dynamics of neutral halogen-containing molecules have been reported. However, relevant ionic species are much less studied. For example, state-resolved photodissociation dynamics of Br_2^+, one of the simplest dihalogen cations, has only been studied in the 3.3−3.7 eV energy region, where the dissociation proceeds via highly vibrationally excited levels of the $A^2\Pi_u$ state above the first dissociation limit [26, 27].

Very recently, we have developed a new experimental instrument that combines the 'state-of-the-art' velocity map imaging technique with a cryogenically cooled ion trap, dedicating for spectroscopy and photodissociation dynamics of gas-phase ionic species in a cold ion beam [28]. Using this instrument, we have experimentally identified the $1^4\Sigma_u^-$ state of Br_2^+ for the first time by [1+1] resonance enhanced two-photon dissociation spectroscopy [29]. Our results also indicate that, for this simple dihalogen cation, considerable spin-orbit couplings between the $1^4\Sigma_u^-$ and $A^2\Pi_u$ states exist.

This work is a follow-up of our recent spectroscopic study on the $A^2\Pi_u$ and $1^4\Sigma_u^-$ states of Br_2^+ [29], and focuses on the state-resolved photodissociation dynamics of mass-selected $^{79}Br_2^+$ in a cold ion beam. The quartet $1^4\Sigma_u^-$ state has been employed as an intermediate state to initiate resonance enhanced two-photon excitation to high-lying dissociative states in the 4.0−5.0 eV energy region above the ground rovibronic state of $^{79}Br_2^+$. The technique of velocity map imaging is employed to measure the quantum-state resolved dissociation channels upon two-photon excitation. The potential role of spin-orbit coupling effect in the dissociation dynamics is also discussed based on our experimental results.

II. EXPERIMENTS

Details of the recently developed cryogenic cylindrical ion trap velocity map imaging (CIT-VMI) spectrometer and experimental procedures are available from Refs.[28, 29]. Br_2^+ ions are generated by 300 eV electron impact ionization of a gas mixture in a supersonic jet expansion formed by a pulsed piezo valve (MassSpecpecD BV). Bromoform molecules ($CHBr_3$, 1%) seeded in 4 bar helium carrier gas are used for the jet expansion. As described in Ref.[29], Br_2^+ ions

*Authors to whom correspondence should be addressed.
E-mail: yangchen@ustc.edu.cn, dzhao@ustc.edu.cn

DOI:10.1063/1674-0068/cjcp1904085

TABLE I Branching ratios r and anisotropy parameters β for individual state-resolved product channels in the intermediate state $1^4\Sigma^-_{u,3/2}$.

λ/nm	v	E	(C-1)		(C-2)		(C-3)+(C-4)		C-5		C-6		C-7	
			r	β	r	β	r	β	r	β	r	β	r	β
628.14	10	3.95	0.009		0.111	+1.59(3)	0.881	+2.00(3)						
594.07	15	4.17			0.433	+1.92(3)	0.567	+1.91(2)						
554.04	22	4.48	0.027	+1.41(36)	0.539	+2.00(8)	0.416	+2.00(9)	0.016		0.001			
539.15	25	4.60			0.015	+2.00(38)	0.024	+2.00(32)	0.961	+2.00(3)				
529.89	27	4.68	0.042	+1.39(39)	0.683	+1.97(12)	0.112	+1.75(38)	0.109	+2.00(15)	0.053	+1.78(19)		
516.84	30	4.80	0.003	+2.00(8)	0.105		0.164	+2.00(6)	0.277	+2.00(4)			0.452	+1.72(1)
504.80	33	4.91					0.012	+2.00(19)	0.694	+2.00(4)			0.295	+2.00(3)

produced in the electron impact ionization plasma are mass-selected by a quadrupole mass filter (QMF, Extrel, HT500) and then injected into a home-made cylindrical ion trap (CIT) that is attached to the second stage cold head of a closed-cycle helium refrigerator. The ion trap, driven by a commercially available radio-frequency (RF) power supply (RM Jordan, D-1203), is used to cool down both kinetic and internal (rotational and vibrational) temperatures of the mass-selected $^{79}Br_2{}^+$ ions. After being trapped for ∼90 ms, the cold ions are then extracted from the trap and form a well-confined ion beam with a kinetic energy of ∼185 eV. The mass selected $^{79}Br_2{}^+$ ions are photolyzed by a loosely focused laser beam in the middle of the repeller and extractor plates of the VMI optics assembly. The photofragmented Br^+ ions are accelerated and projected onto a position-sensitive imaging detector consisting of two 75 mm diameter microchannel plates (MCPs) and a P20 phosphor screen (Photek, VID275). By applying a fast high-voltage switch on one of the MCPs for mass selection and detection gating, the two-dimensional velocity distributions of photofragmented Br^+ ions are imaged by the technique of DC-slice VMI. The transient images on the phosphor screen are captured by an electron multiplying charge coupled device (EMCCD) camera (Andor, iXon Ultra 888, 1024×1024 pixels) and transferred to a computer on every shot for event-counting and image processing.

The fundamental output of a pulsed dye laser (Sirah, PrecisionScan) pumped by a Nd:YAG laser (Spectra-Physics, Quanta Ray Pro-250) is employed as the photolysis light source. The direction of the electric vector of the polarized dye laser is set perpendicular to the ion beam and parallel to the MCP detector plane. Typically, the dye laser beam is set at ∼2 mJ/pulse and is loosely focused by a lens (f=450 mm) before entering the vacuum chamber.

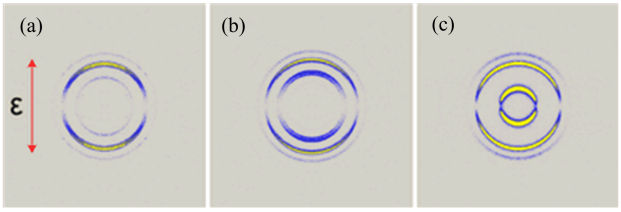

FIG. 1 Experimental images of $^{79}Br^+$ recorded from two-photon dissociation of $^{79}Br_2{}^+$ with laser wavelengths at (a) 554.04 nm, (b) 529.89 nm, and (c) 504.83 nm, respectively. Red arrow in the left of the images indicates the polarization direction of the photolysis laser.

III. RESULTS AND DISCUSSION

We have measured DC-sliced images of photofrgmented $^{79}Br^+$ ions at seven different wavelengths (see Table I). All photolysis wavelengths are selected at resonant positions of the $1^4\Sigma^-_{u,3/2}$-$X^2\Pi_{g,3/2}$ electronic transition bands of $^{79}Br_2{}^+$, ensuring that only $^{79}Br^+$ ions in the spin-orbit ground state $X^2\Pi_{g,3/2}$ are photodissociated in our experiments. FIG. 1 shows the experimental images at three selected wavelengths with vibrational levels of v=22, 27, and 33 in the $1^4\Sigma^-_{u,3/2}$ intermediate state. Each image displays a two-dimensional recoiling velocity (speed and angular) distributions of photofragmented $^{79}Br^+$ atoms. Since the co-frgmented neutral ^{79}Br has nearly the same mass as the ionic $^{79}Br^+$, according to the the momentum conservation in the dissociation process, neutral ^{79}Br atoms are of the same velocity distributions as $^{79}Br^+$ at each laser wavelength. Consequently, total kinetic energy release (TKER) can be obtained from the velocity distributions of $^{79}Br^+$ that can be determined from our experimental images. In FIG. 2, example TKER spectra are presented. The peaks in each TKER spectrum, corresponding to the well-resolved ring structures in the experimental images, reflect information of state-resolved photodissociation dynamics.

In the 630−500 nm wavelength region studied here, single-photon energy (2.0−2.5 eV) is not sufficient to

DOI:10.1063/1674-0068/cjcp1904085

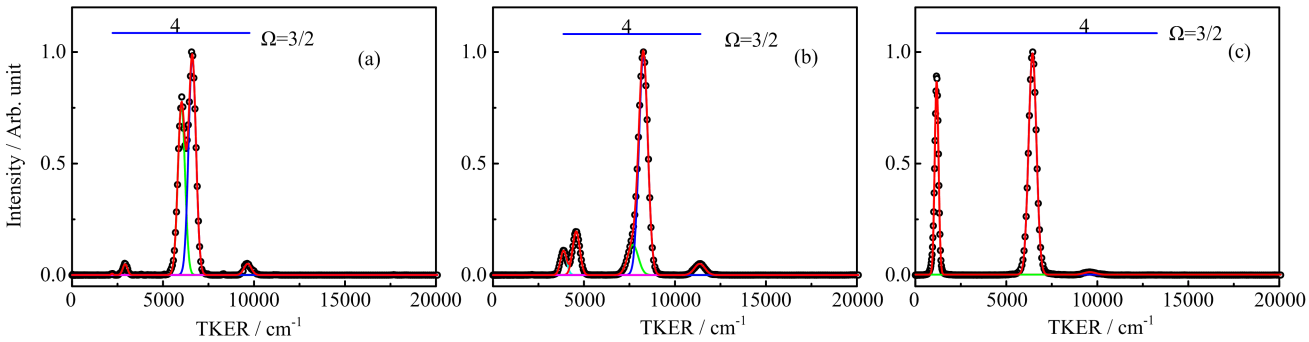

FIG. 2 The total kinetic energy release (TKER) spectra (circles) from two-photon dissociation of $^{79}Br_2^+$ at (a) 554.04 nm, (b) 529.89 nm, and (c) 504.83 nm, respectively. Corresponding experimental images of the photofragmented Br^+ ions are given in FIG. 1. Assignments of possible dissociation channels (C-i) are marked on the top of each panel. Fitted curves of the TKER spectra using Gaussian function are illustrated with solid traces.

dissociate $^{79}Br_2^+$, and photofragmentation of $^{79}Br_2^+$ proceeds via resonance enhanced [1+1] two-photon excitation process. Possible state-resolved dissociation channels are:

$$^{79}Br_2^+\left(X^2\Pi_{g,3/2}\right)+[1+1]h\nu\rightarrow {}^{79}Br^+\left(^3P_2\right)+{}^{79}Br\left(^2P_{3/2}\right) \quad \text{(C-1)}$$

$$^{79}Br_2^+\left(X^2\Pi_{g,3/2}\right)+[1+1]h\nu\rightarrow {}^{79}Br^+\left(^3P_1\right)+{}^{79}Br\left(^2P_{3/2}\right) \quad \text{(C-2)}$$

$$^{79}Br_2^+\left(X^2\Pi_{g,3/2}\right)+[1+1]h\nu\rightarrow {}^{79}Br^+\left(^3P_2\right)+{}^{79}Br\left(^2P_{1/2}\right) \quad \text{(C-3)}$$

$$^{79}Br_2^+\left(X^2\Pi_{g,3/2}\right)+[1+1]h\nu\rightarrow {}^{79}Br^+\left(^3P_0\right)+{}^{79}Br\left(^2P_{3/2}\right) \quad \text{(C-4)}$$

$$^{79}Br_2^+\left(X^2\Pi_{g,3/2}\right)+[1+1]h\nu\rightarrow {}^{79}Br^+\left(^3P_1\right)+{}^{79}Br\left(^2P_{1/2}\right) \quad \text{(C-5)}$$

$$^{79}Br_2^+\left(X^2\Pi_{g,3/2}\right)+[1+1]h\nu\rightarrow {}^{79}Br^+\left(^3P_0\right)+{}^{79}Br\left(^2P_{1/2}\right) \quad \text{(C-6)}$$

$$^{79}Br_2^+\left(X^2\Pi_{g,3/2}\right)+[1+1]h\nu\rightarrow {}^{79}Br^+\left(^1D\right)+{}^{79}Br\left(^2P_{3/2}\right) \quad \text{(C-7)}$$

The energy conservation in the [1+1] two-photon dissociation reaction can be written as:

$$E_T = 2h\nu - D_i \quad (1)$$

where E_T is the total kinetic energy of photofragments, and D_i is (i=1−7) the dissociation threshold for individual dissociation channels (C-i). Based on available atomic level energies [26], values of D_i (i=1−7) are determined as 26345, 29481, 30030, 30183, 33167, 33868, and 38434 cm^{-1} for C-i (i=1−7), respectively. Using Eq.(1), assignments of the observed peaks in the TKER spectra to individual dissociation channels can be straightforwardly obtained by comparisons with the calculated TKER values (see FIG. 2). As have been discussed in our recent spectroscopic study [29], the peak intervals in the TKER spectra, as well as the accurate dissociation limits given above, also provide an additional check for the assignments of the ground spin-orbit quantum number Ω.

Using the TKER spectra and corresponding assignments, we have performed least square fits by linear combination of Gaussian function and determined the branching ratios of individual product channel. The results are summarized in Table I. It can be seen that, contributions of the (C-1) and (C-6) channels are nearly negligible at all wavelengths. For the (C-7) channel, it is observable with considerable contributions immediately after the total excitation energy exceeds its dissociation limit (4.77 eV).

Angular distributions of individual product channels are also obtained by integrating the velocity distribution over an appropriate range as a function of the angle (θ) between the laser polarization and the recoiling velocity of the photofragments. Individual angular distributions are fitted using the following equation:

$$I(\theta) \propto 1 + \beta P_2(\cos\theta) \quad (2)$$

where the term $P_2(\cos\theta)$ is the second-order Legendre polynomial, and β is the anisotropy parameter [30]. For a fast dissociation process, the parameter β has a physical range between −1 and +2, with the minimum limiting value of −1 corresponding to excitation via a perpendicular transition, and the maximum limiting value of +2 corresponding to excitation via a pure parallel transition. In FIG. 3, example analysis of the angular distributions for the 504.87 nm image is presented. The resulting β values for all experimental images have been summarized in Table I. It is noted here that the obtained branching ratios for the (C-1) channel at all wavelengths are small, probihiting accurate fits of the angular distributions. In our analysis, only two β values for the (C-1) channel at 554.04 and 529.89 nm, respectively, are derived, which may have errors larger than the statistical uncertainties given in Table I.

It can be seen from Table I that nearly all obtained

DOI:10.1063/1674-0068/cjcp1904085

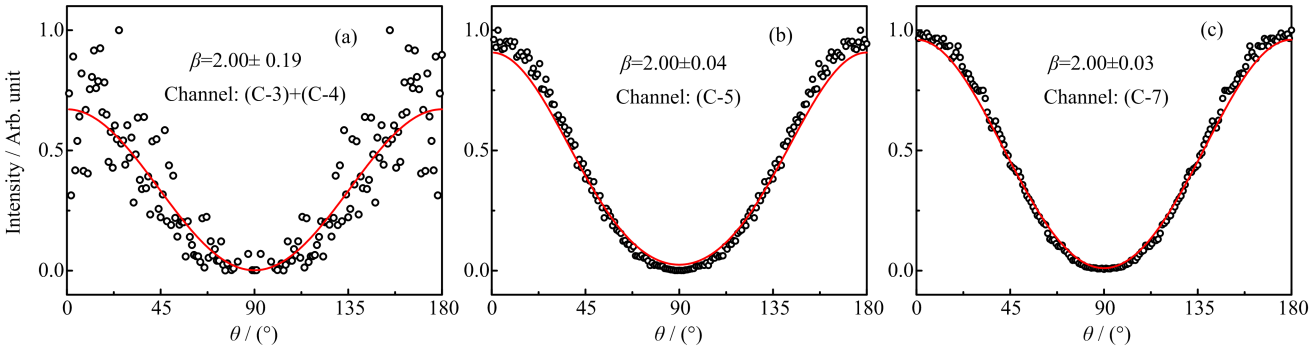

FIG. 3 Experimental and fitted angular distributions of the fragmented Br^+ ion from two-photon dissociation of $^{79}Br_2{}^+$ at 504.83 nm for production channels (a) (C-3)+(C-4), (b) (C-5), and (c) (C-7), respectively. The derived anisotropy parameters β determined from least square fits are also given.

anisotropy parameters β are close/equal to the maximum limiting value +2. In the present experiment, the parent $^{79}Br_2{}^+$ ions are dissociated via resonance enhanced [1+1] two-photon excitation. We have shown in Ref.[29] that, in the first step of resonant excitation, the intermediate quartet state $1^4\Sigma^-_{u,3/2}$ is accessed by "intensity borrowing" via strong spin-orbit coupling with the $A^2\Pi_u$ state. The intermediate quartet state $1^4\Sigma^-_{u,3/2}$ is expected to have a lifetime at least comparable to that for the $A^2\Pi_u$ state, which has been known to be 1−10 μs. In this case, the two-photon dissociation can be approximated as a single-photon processes of excited $^{79}Br_2{}^+$ at its $1^4\Sigma^-_{u,3/2}$ state. In other words, the measured anisotropy parameters β listed in Table I indicate that the photoexcitation transitions from the intermediate $1^4\Sigma^-_{u,3/2}$ state to higher dissociative states are parallel type transitions.

So far, no theoretical calculations on the excited states of $Br_2{}^+$ in the 4.0−5.0 eV energy region are available. In Ref.[31], a higher-lying $^2\Sigma^+_g$ state with an avoided crossing is suggested to be responsible for the dissociation process. However, this $^2\Sigma^+_g$ state cannot explain the anisotropy parameters β obtained in our experiment, because the transitions from either the $^4\Sigma^-_{u,3/2}$ intermediate state or the mixed $A^2\Pi_u, 3/2$ state to $^2\Sigma^+_g$ should be perpendicular type transitions. On the other hand, early theoretical calculations [32, 33] and our spectroscopic identification of the $^4\Sigma^-_{u,3/2}$ state have proven that the spin-orbit coupling effects in $Br_2{}^+$ are considerably strong. In the higher energy region of 4.0−5.0 eV, the spin-orbit coupling and mixing may be more pronounced due to higher state density, and likely, only the spin-orbit quantum (Ω) can be effectively resolved. Our experimental results indicate that photofragmentation occurs from Ω=3/2 dissociative excited states via $\Delta\Omega$=0 parallel transitions. Other than the previously proposed $^2\Sigma^+_g$ state, one or more higher-lying dissociative quartet states are likely involved. High level theoretical investigations on the spin-orbit resolved excited states of $Br_2{}^+$ are desired to get a more in-depth understanding of the present experimental results.

IV. CONCLUSION

Total kinetic energy release spectra and photofragment angular distributions have been experimentally measured for the [1+1] two-photon dissociation dynamics of mass-selected $^{79}Br_2{}^+$ ions in the 4.0−5.0 eV excitation energy region above the ground rovibronic state. Quantum state resolved product channels have been observed and corresponding branching ratios are experimentally determined. The measured photofragment angular distributions indicate that photofragmentation occurs from Ω=3/2 dissociative excited states via $\Delta\Omega$=0 parallel transitions. Due to the considerable spin-orbit coupling effects in the excited states of $^{79}Br_2{}^+$, higher-lying dissociative quartet states are likely responsible for the observed photodissociation processes.

V. ACKNOWLEDGEMENTS

This study was supported by the National Natural Science Foundation (No.21773221 and No.21827804), the National Key R&D Program of China (2017YFA0303502), and Fundamental Research Funds for the Central Universities of China (WK2340000078).

[1] C. George, M. Ammann, B. D'Anna, D. Donaldson, and S, A. Nizkorodov, Chem. Rev. **115**, 4218 (2015).
[2] W. R. Simpson, S. S. Brown, A. Saiz-Lopez, J. A. Thornton, and R. von Glasow, Chem. Rev. **115**, 4035 (2015).
[3] B. J. Finlayson-Pitts, Anal. Chem. **82**, 770 (2010).
[4] R. S. Mulliken, J. Chem. Phys. **3**, 514 (1935).

DOI:10.1063/1674-0068/cjcp1904085

[5] A. Saiz-Lopez and R. von Glasow, Chem. Soc. Rev. **41**, 6448 (2012).
[6] M. N. Ashfold, G. A. King, D. Murdock, M. G. Nix, T. A. Oliver, and A. G. Sage, Phys. Chem. Chem. Phys. **12**, 1218 (2010).
[7] A. G. Sage, T. A. Oliver, D. Murdock, M. B. Crow, G. A. Ritchie, J. N. Harvey, and M. N. Ashfold, Phys. Chem. Chem. Phys. **13**, 8075 (2011).
[8] G. Pino, A. Oldani, E. Marceca, M. Fujii, S. I. Ishiuchi, M. Miyazaki, M. Broquier, C. Dedonder, and C. Jouvet, J. Chem. Phys. **133**, 124313 (2010).
[9] K. C. Lin and P. Y. Tsai, Phys. Chem. Chem. Phys. **16**, 7184 (2014).
[10] A. Abdel-Hafiez, R. Atteya, and M. Medhat, Int. J. Phys. Sci. **5**, 978 (2010).
[11] M. Chen, H. Liang, C. He, D. F. Zhao, and Y. Chen, Chin. J. Chem. Phys. **31**, 563 (2018).
[12] S. F. Chen, F. Y. Liu, and Y. J. Liu, J. Chem. Phys. **131**, 124304 (2009).
[13] M. Cheng, D. Lin, L. Hu, Y. Du, and Q. Zhu, Phys. Chem. Chem. Phys. **18**, 3165 (2016).
[14] K. S. Dooley, J. N. Geidosch, and S. W. North, Chem. Phys. Lett. **457**, 303 (2008).
[15] C. Escure, T. Leininger, and B. Lepetit, J. Chem. Phys. **130**, 244305 (2009).
[16] D. Karlsson and J. Davidsson, J. Photochem. Photobiol. A **195**, 242 (2008).
[17] A. Kumar, E. C. Lee, S. Lee, and M. Kołaski, Chem. Phys. Lett. **482**, 189 (2009).
[18] W. G. Merrill, F. F. Crim, and A. S. Case, Phys. Chem. Chem. Phys. **18**, 32999 (2016).
[19] D. Murdock, M. B. Crow, G. A. Ritchie, and M. N. Ashfold, J. Chem. Phys. **136**, 124313 (2012).
[20] M. L. Murillo-Sánchez, S. M. Poullain, J. J. Bajo, M. E. Corrales, J. González-Vázquez, I. R. Solá, and L. Bañares, Phys. Chem. Chem. Phys. **20**, 20766 (2018).
[21] C. Pan, Y. Zhang, J. D. Lee, and N. M. Kidwell, J. Phys. Chem. A **122**, 3728 (2018).
[22] A. G. Smolin, O. S. Vasyutinskii, G. G. Balint-Kurti, and A. Brown, J. Phys. Chem. A **110**, 5371 (2006).
[23] M. Sumida, T. Hanada, K. Yamasaki, and H. Kohguchi, J. Chem. Phys. **141**, 104316 (2014).
[24] S. Woittequand, C. Toubin, M. Monnerville, S. Briquez, B. Pouilly, and H. D. Meyer, J. Chem. Phys. **131**, 194303 (2009).
[25] X. P. Zhang, Z. R. Wei, Y. Tang, T. J. Chao, B. Zhang, and K. C. Lin, Chem. Phys. Chem. **9**, 1130 (2008).
[26] M. Beckert, S. J. Greaves, and M. N. R. Ashfold, Phys. Chem. Chem. Phys. **5**, 308 (2003).
[27] O. P. J. Vieuxmaire, M. G. D. Nix, J. A. J. Fitzpatrick, M. Beckert, R. N. Dixon, and M. N. R. Ashfold, Phys. Chem. Chem. Phys. **6**, 543 (2004).
[28] Z. Hua, S. Feng, Z. Zhou, H. Liang, Y. Chen, and D. Zhao, Rev. Sci. Instrum. **90**, 013101 (2019).
[29] H. Liang, Z. Zhou, Z. Hua, Y. Zhao, S. Feng, Y. Chen, and D. Zhao, J. Phys. Chem. A **123**, 4609 (2019).
[30] P. L. Houston, J. Phys. Chem. **91**, 5388 (1987).
[31] R. McLoughlin, J. Morrison, and D. Smith, Int. J. Mass. Spectro. **58**, 201 (1984).
[32] K. Balasubramanian, Chem. Phys. **119**, 41 (1988).
[33] K. Balasubramanian, Chem. Rev. **90**, 93 (1990).

DOI:10.1063/1674-0068/cjcp1904085